ACS OMEGA

Article

Cite This: ACS Omega 2019, 4, 19096−19105

http://pubs.acs.org/journal/acsodf

Proteomic Analysis of the Xanthan-Degrading Pathway of *Microbacterium* sp. XT11

Zhen Sun, Huixue Liu,† Xueyan Wang,† Fan Yang,* and Xianzhen Li*

School of Biological Engineering, Dalian Polytechnic University, Dalian 116034, Liaoning, PR China

Supporting Information

ABSTRACT: Xanthan, a highly stable polysaccharide which is not easily degraded by most microorganisms, contains a cellulosic backbone with trisaccharide side chains composed of mannosyl-glucuronyl-mannose attached α-1,3 to alternating glucosyl residues. Different digestion strategies were first applied to demonstrate the complexity about the proteomes of *Microbacterium* sp. XT11 in xanthan medium and glucose medium. Significantly up-regulated proteins induced by xanthan were screened out by the label-free quantitation of the proteomes of *Microbacterium* sp. XT11 in xanthan medium and glucose medium. Consequently, 2746 and 2878 proteins were identified in proteomes of *Microbacterium* sp. XT11 in xanthan medium and glucose medium individually, which represent 80.6 and 84.4% of total protein dataset predicted to be expressed by the gene. In the list of 430 induced proteins containing the proteins specifically expressed or up-regulated in xanthan medium, 19 proteins involved in carbohydrate-active enzymes database and 38 proteins annotated with transporter activity were critical in the degrading pathway of xanthan. Four CAZymes (GH3, GH38, GH9, and PL8) and one ABC transporter (LX1-1GL001097) were verified with quantitative real-time polymerase chain reaction. Four CAZymes (GH3, GH38, GH9, and PL8) were further verified with the enzyme assay. This study suggests a xanthan-degrading pathway in *Microbacterium* sp. XT11, and other potential xanthan degradation-related proteins still need further investigation.

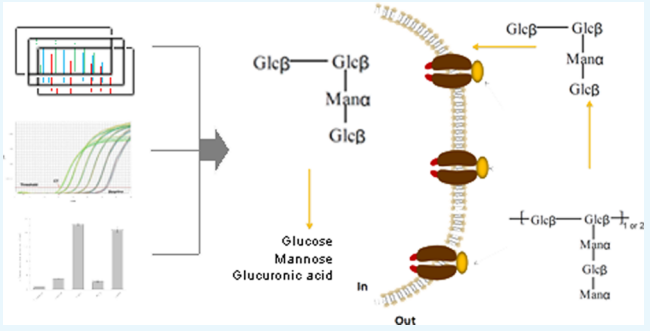

INTRODUCTION

Xanthan is an important extracellular heteropolysaccharide produced by a plant-pathogenic bacterium, *Xanthomonas campestris* pv. *campestris*.[1] This polysaccharide has a cellulosic backbone with trisaccharide side chains composed of mannosyl-glucuronyl-mannose attached α-1,3 to alternating glucosyl residues.[2] The internal mannosyl residues are acetylated and the terminal mannosyl residues are pyruvated in the side chain, but the extent of modification varies with xanthan-producing strains and culture conditions.[3] Because of superior rheological properties, xanthan has been widely used in the food, pharmaceutical, and oil industry as the thickener, gelling, and stabilizing agent.[4−6]

Interestingly, xanthan is considered to play a key role in the virulence of *Xanthomonas* bacterial cells in causing black rot,[7] but its degradation product could inhibit *X. campestris* pv. *campestris*.[8] Additionally, the xanthan with truncated side chain is very useful in altering the viscosity of suspensions injected into the underground oil-bearing formations.[9] However, xanthan is a highly stable polysaccharide which is not easily degraded by most microorganisms. Only a few of microorganisms and related enzymes have been reported to participate in the depolymerization of the polysaccharide.[10−13] The first complete report on xanthan degradation by bacteria was done by Nankai et al., in which an enzymatic route for the degradation of xanthan in *Bacillus* sp. strain GL1 by analyzing the structures of xanthan depolymerization products was elucidated.[14]

In our previous work, an excellent xanthan-degrading bacterium *Microbacterium* sp. XT11 was isolated.[15] Xanthan lyase and endoxanthanase produced by *Microbacterium* sp. XT11 were purified and characterized.[16,17] Yang et al. reported a high-quality complete genome sequence of a xanthan-degrading bacterium *Microbacterium* sp. XT11, and four genes probably involved in xanthan-degradation pathway were detected as a gene cluster in the genome.[18] However, the proteins involved in the degradation process of xanthan were not yet simultaneously analyzed. As we all know, the defence response in plant cells mediated by elicitor molecules could help plants to resist infective diseases.[19] Xanthan is the most favorable carbon resource for both the growth and enzyme production of *Microbacterium* sp. XT11. Some oligosaccharides of xanthan were confirmed to directly inhibit *Xanthomonas* bacterium and be elicitor-active that could induce the accumulation of phytoalexin in the soybean cotyledon in our previous experiment.[15] As the separation or the chemical synthesis of elicitor-active oligosaccharide of xanthan was hard, the controllable enzymatic degradation of xanthan may be an

Received: July 24, 2019
Accepted: October 23, 2019
Published: November 6, 2019

DOI: 10.1021/acsomega.9b02313
ACS Omega 2019, 4, 19096−19105

alternative method. Therefore, all the related proteins involved in the degradation of xanthan were worth studying.

Mass spectrometry (MS) has become an essential tool in all biological research, most remarkably by enabling the large-scale identification, characterization, and quantification of proteins.[20,21] MS-based proteomics is the systematic study of the many and diverse properties of proteins in a parallel manner in biological systems.[22] Currently, the shotgun proteomics strategy became the first choice for identifying proteins in most large-scale studies, which was based on digesting proteins into peptides and sequencing them using tandem MS and automated database searching.[23] Therefore, protein identification and proteome sequence coverage can be efficiently improved by using multiple proteases with complementary cleavage specificities.[24,25] In our research, the digestion strategy with multiple proteases was first applied to extend knowledge about the proteomes of *Microbacterium* sp. XT11 in xanthan medium and glucose medium. Then, the differential analysis of the proteomes of *Microbacterium* sp. XT11 in xanthan medium and glucose medium was carried out by the label-free quantitation (LFQ) strategy to explore the significantly changed proteins induced by xanthan. All the induced proteins related with xanthan biodegradation were referenced for GO-annotation and carbohydrate-active enzymes database (CAZy) to find out carbohydrate-active enzymes and proteins with transporter activity, which was critical in the xanthan-degrading pathway. Finally, the selected proteins were further verified with quantitative real-time polymerase chain reaction (PCR) and enzyme assay.

RESULTS AND DISCUSSION

***Microbacterium* sp. XT11 Grew Well in Xanthan Medium and Glucose Medium.** *Microbacterium* sp. XT11 was identified as the bacteria capable of fragmenting xanthan. It was confirmed that various carbohydrates used as carbon sources supported the growth of strain XT11.[15] Therefore, the proteins related with xanthan bio-degradation may be induced by xanthan. As shown in Figure 1, strain XT11 grew well when cultured in xanthan medium and the cell mass (OD_{600}) can be up to 4. It took less than 25 h to reach the stationary phase. The bacteria also grew well with glucose as the carbon source in medium and the cell mass (OD_{600}) was up to 3 when the stationary phase was reached within 12 h. Hence, the proteomes of strain XT11 when cultured in xanthan medium and glucose medium were compared to investigate the proteins related with xanthan biodegradation. The proteome of strain XT11 when cultured in glucose medium was used as the control experiment.

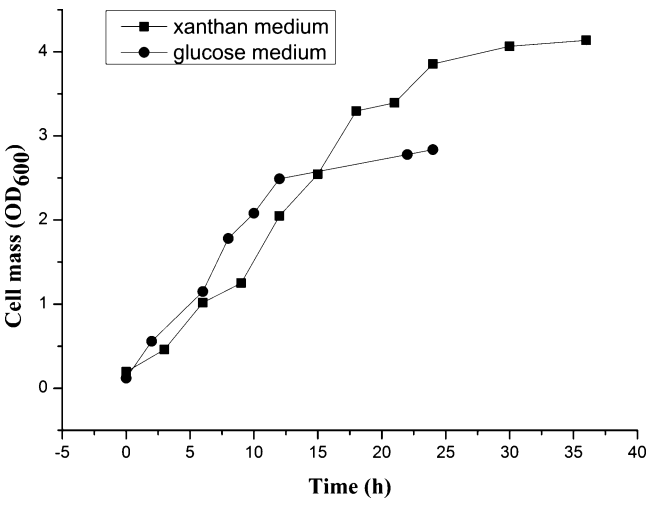

Figure 1. Grow curve of *Microbacterium* sp. XT11 in xanthan medium and glucose medium.

Multiple Protease Digestion Revealed the Complicated Proteomes of *Microbacterium* sp. XT11. Considering the fact that amino acids composition varied among different proteins, proteases with different cleavage specificity can be applied to increase the sequence coverage of protein analysis. As chymotrypsin has complementary cleavage specificity to trypsin, it can be expected that many proteins which cannot be identified by trypsin digestion are possibly to be identified by chymotrypsin digestion. In addition, the combined use of trypsin and chymotrypsin not only efficiently takes advantage of the complementary cleavages of chymotrypsin relative to trypsin but also improves the identification of the long peptide. Therefore, the proteins expressed by strain XT11 in xanthan medium and glucose medium which were designated as proteome I and II, respectively, were all analyzed by using three different digestion strategies (trypsin, chymotrypsin, and trypsin and chymotrypsin) (Figure 2).

Both proteome I and II can be divided into two parts: one was identified from whole cell lysate (cell protein) and another was identified in the medium with the signal peptide (extracellular protein). Secretory signal peptides were predicted by the SignalP 4.1 server.[26] For cell protein, trypsin digestion led to the identification of 2084 and 2022 proteins in proteome I and II individually, while the total number of identified proteins reached 2553 and 2684 by using other two digestion strategies (Figure 3A,C). For extracellular protein, 143 and 146 proteins were detected by using trypsin digestion in proteome I and II, respectively, while, in total, 193 and 194 proteins were detected combined with other two digestion strategies (Figure 3B,D). The number increased by 22.5, 32.7, 35.0, and 32.9%, individually. As described by Biringer et al., combining data from two individual digests produced by different proteases significantly enhanced the overall sequence coverage for most cerebrospinal fluid proteins and aided in protein identification.[24] Our results further supported that the use of complementary proteases improved the proteome coverage remarkably. Totally, 3409 genes of *Microbacterium* sp. XT11 were sequenced. Combining the data of two parts, 2746 and 2878 proteins were identified in proteome I and II individually, which represented 80.6 and 84.4% of total protein dataset expressed by the gene. The large proportion of identification in total protein dataset confirmed the reliability of our experiment.

Label-Free Quantification Strategy Explored the Induced Proteins Related with Xanthan Biodegradation. As mentioned above, 229 and 361 proteins were specifically expressed individually in the identified 2746 and 2878 proteins of proteome I and II (detailed information of 229 and 361 proteins were listed in the Tables S1 and S2 in the Supporting Information). These proteins were either identified in proteome I or in proteome II, so these proteins were specific proteins closely related with culture medium. Apart from these specific proteins, proteins highly expressed when cultured in xanthan medium relative to glucose medium were also considered as induced proteins related with xanthan biodegradation. Therefore, the LFQ strategy based on the analysis of the peak area of precursor ions, which did not have

DOI: 10.1021/acsomega.9b02313
ACS Omega 2019, 4, 19096−19105

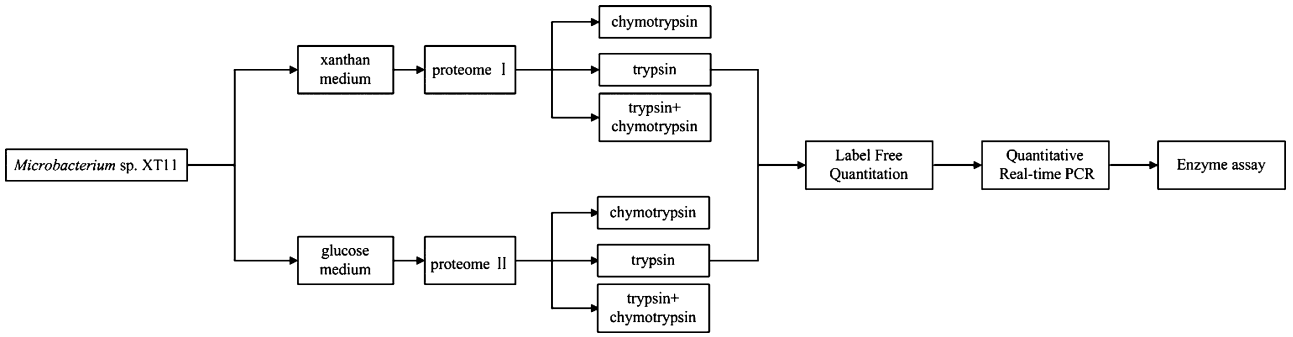

Figure 2. Work flow for analysis of the xanthan-degrading bacterium *Microbacterium* sp. XT11 proteome and the induced proteins related with xanthan bio-degradation.

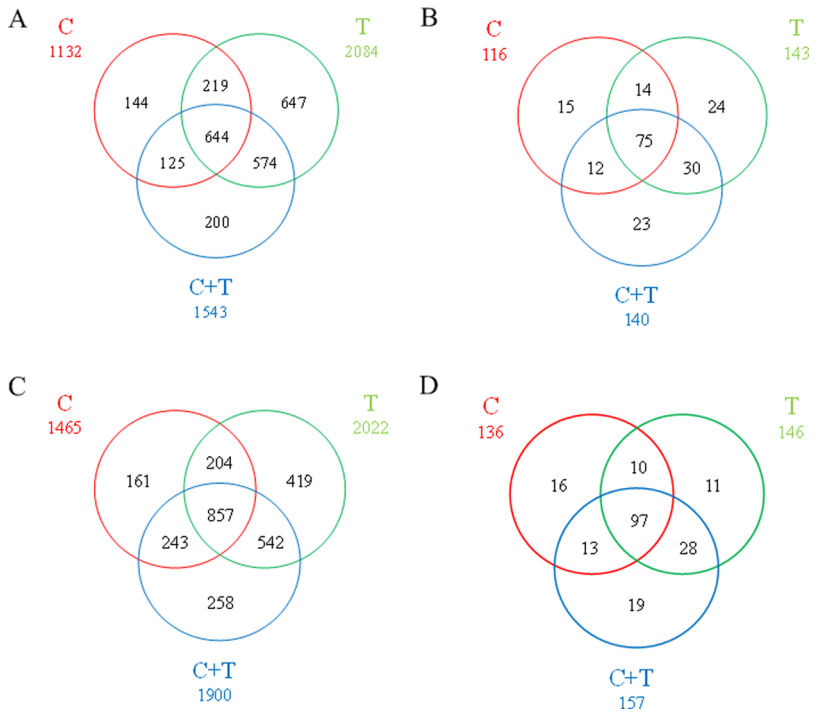

Figure 3. Venn diagram showing the overlap of the identified cell protein in proteome I (A) and II (C) by using three digestion strategy (trypsin, T for short; chymotrypsin, C for short; trypsin & chymotrypsin, T + C for short). The venn diagram showing the overlap of the identified extracellular protein in proteome I (B) and II (D) by using three digestion strategy (trypsin, T for short; chymotrypsin, C for short; trypsin & chymotrypsin, T + C for short).

a time-consuming step of isotopic labeling,[27] was applied to comparatively analyze the proteomes of *Microbacterium* sp. XT11 in xanthan medium and glucose medium, to explore the significantly up-regulated proteins induced by xanthan. LC/MS/MS results of three biological replicates were merged together for LFQ analysis. When the expression level of a protein showed a twofold change in abundance compared to the control ($q < 0.05$), the protein was considered to be significantly up-regulated. The ratios were described as abundance ratios (proteome I/proteome II). When *Microbacterium* sp. XT11 in glucose medium was considered as the control, *Microbacterium* sp. XT11 in xanthan medium displayed 179 higher expression cell proteins and 36 higher expression extracellular proteins (detailed information of 179 and 36 proteins were listed in the Tables S3 and S4 in the Supporting Information). Considering the fact that low abundance protein cannot be stably identified in each run of MS, the proteins specifically expressed or up-regulated when cultured in xanthan medium by removing the redundant proteins in these two parts were considered as the induced proteins related with xanthan biodegradation. Finally, 430 proteins were classified as the induced proteins related with xanthan biodegradation.

To reveal the main functions of the induced proteins related with xanthan biodegradation, these proteins of which 251 were GO-annotated were categorized functionally into three large groups including molecular functions, biological processes, and cellular components by using the WEGO (Web Gene Ontology Annotation Plot) web service (http://wego.genomics.org.cn/).[28] As shown in Figure 4, these GO-annotated proteins were distributed among 24 subgroups, in which each of the categories of "catalytic activity", "binding", "cellular process" and "metabolic process" contained more than 30% proteins. In contrast, relatively few proteins (more than 10% proteins) were contained in the categories of "cell part", "cell", "membrane", "transporter activity", "transcription regulator activity", "localization", "biological regulation", and

DOI: 10.1021/acsomega.9b02313
ACS Omega 2019, 4, 19096−19105

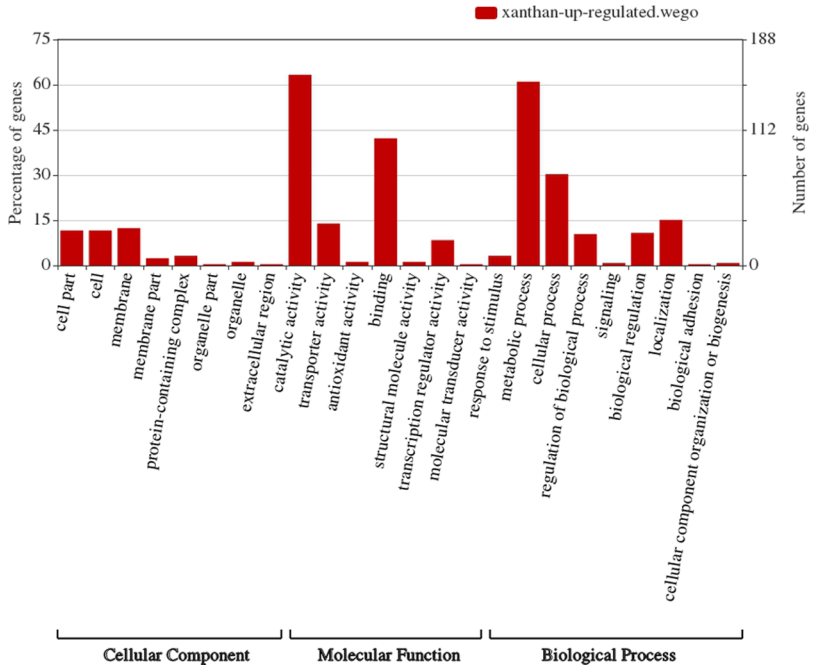

Figure 4. Bar graph showing the distribution of the percentage of GO-annotated protein with cellular component, molecular function and biological process. Exactly as some proteins have multiple subcellular locations, a great number of proteins are associated with diverse molecular functions and involved in various biological processes. Therefore, the sum of all the subcategories with GO annotation must exceed 100%.

"regulation of biological process". Apart from abovementioned categories, other categories displayed very few proteins.

Carbohydrate-Active Enzymes and Proteins with Transporter Activity Played Critical Roles in Xanthan-Degrading Process. Considering the fact that the complete degradation of xanthan needs both the intracellular and extracellular enzymatic process, carbohydrate-active enzymes and proteins with transporter activity should be critical in the process. Therefore, all the induced proteins related with xanthan bio-degradation were referenced for GO-annotation and CAZy to find out carbohydrate-active enzymes and proteins with transporter activity. For the novel proteins without functional annotation, their functions were referred to the highly homologous protein (>95%) which was sought out by blasting in the existed database with the amino acid sequences of proteins.[29] In the induced protein list, 19 proteins were involved in CAZy and 38 proteins were annotated with transporter activity (Table 1).

GH3 was expressed as cell protein and 21.6 times more in proteome I than in proteome II. GH38 which was responsible for hydrolysis of disaccharide to mannose and glucose was also detected to be increased 4.9-fold. GH9 and PL8 which were both detected with a signal peptide were 68.6 and 27.4 times individually more in proteome I than in proteome II. Obviously, GH3, GH9, GH38, and PL8 which can be cooperative to depolymerize xanthan from pentasaccharide to disaccharide were highly expressed when xanthan was supplemented in the medium.

We have previously confirmed the function of PL8 in the xanthan-degrading pathway that PL8 (xanthan lyase, protein ID LX1-1GL001102) was specific on the pyruvated mannosyl residue in the intact xanthan molecule.[17] GH9 (endoglucanase, protein ID LX1-1GL001095) was newly characterized as endo-type xanthanase efficiently and randomly cleaving glucosidic bonds within the backbone of highly ordered xanthan, of which the specific activity on xanthan was significantly higher than other known GH9 cellulases on CMC.[30] Additionally, the carbohydrate-binding module (CBM) in extracellular enzymes (GH9 and PL8) could specifically recognize and bind to xanthan chains, leading to subsequent degradation of xanthan, when XT11 was cultured in xanthan medium.[17,30]

An ATP-binding cassette (ABC)-type sugar transport complex (protein ID LX1-1GL001097, LX1-1GL001098, LX1-1GL001099) was reported to be located in the cluster with four CAZymes and presumably plays a role in transporting oligosaccharides into cells.[18,31] In our research, LX1-1GL001097 was detected with a signal peptide and was 100 times more in proteome I than in proteome II. Meanwhile, LX1-1GL001098 was detected in the cell part and its amount increased 100 times when xanthan was supplemented. However, LX1-1GL001099 was detected as cell protein only with chymotrypsin as the protease. As the frequencies of lysine and arginine appeared in LX1-1GL001099 were low and their distributions were uneven among the sequence of amino acids, the mass of tryptic peptides rarely fell into the scan range of MS. Therefore, LX1-1GL001099 was not quantified by tryptic digestion.

These four CAZymes and an ABC-type sugar transport complex were found to be located in a cluster under the control of a transcriptional regulator in *Microbacterium* sp. XT11.[18] Moreover, the structures of xanthan depolymerization products were determined by Nankai et al.[14] Therefore, we suggested a xanthan-degrading pathway in *Microbacterium* sp. XT11 according to the abovementioned results of proteomic analysis. The variation trend and subcellular location of four CAZymes and two ABC transporters supported the putative xanthan-degrading pathway in *Microbacterium* sp. XT11 that xanthan was extracellularly degraded to tetrasaccharides, then transported into cells through ABC-transporters, finally intracellularly cleaved into glucose, mannose, and glucuronate (Figure 5). This suggested that the xanthan-degrading pathway was in accordance with the enzymatic route for the

DOI: 10.1021/acsomega.9b02313
ACS Omega 2019, 4, 19096−19105

Table 1. Detailed Information of 19 Proteins Involved in CAZy and 38 Proteins Annotated with Transporter Activity Which Were in the List of Induced Proteins Related with Xanthan Bio-Degradation

protein name/Blast result	family	abundance ratio	identified location
hypothetical protein [*Microbacterium* sp. UCD-TDU]	GH13	100	cell
hypothetical protein [*Microbacterium* sp. UCD-TDU]	GHO	specific	cell
hypothetical protein [*Microbacterium yannicii*]	GH13	100	cell
hypothetical protein [*Microbacterium* sp. 292MF]	GH13	53.434	extracellular
alpha-mannosidase [*Microbacterium* sp. UCD-TDU]	GH38	100	cell
hypothetical protein [*Microbacterium* sp. UCD-TDU]	GH5	specific	cell
hypothetical protein [*Microbacterium testaceum*]	GH9	68.626	extracellular
Xylan 1, 4-beta-xylosidase [*Actinosynnema mirum* DSM 43827]	GH3	21.562	cell
alpha-mannosidase [*M. testaceum*]	GH38	4.945	cell
beta-D-glucosideglucohydrolase [*Microbacterium* sp. UCD-TDU]	GH3	2.116	cell
alpha-glucosidase [*Microbacterium* sp. UCD-TDU]	GH13	2.098	cell
hypothetical protein [*Microbacterium barkeri*]	GH13	3.213	cell
hypothetical protein [*M. barkeri*]	GH29	2.043	cell
alpha-glucosidase, family 31 of glycosyl hydrolase [*M. testaceum*]	GH31	4.868	extracellular
hypothetical protein [*M. testaceum*]	PL8	27.354	extracellular
proline iminopeptidase [*Microbacterium* sp. UCD-TDU]	GT2	2.89	cell
hypothetical protein [*Microbacterium* sp. UCD-TDU]	GT4	specific	cell
hypothetical protein [*Microbacterium* sp. UCD-TDU]	CBM5	100	cell
hypothetical protein [*Microbacterium* sp.]	GT2	specific	cell
ATPase [*M. barkeri*]	ATPase component	3.326	cell
ATPase [*Microbacterium* sp. UCD-TDU]	ATPase component	specific	cell
ABC transporter ATP-binding protein [*Mycobacterium* sp. VKM Ac-1815D]	ATPase component	2.168	cell
iron-dicitrate ABC transporter ATP-binding protein [*M. barkeri*]	ATPase component	12.255	cell
ABC transporter related protein [*Xylanimonas cellulosilytica* DSM 15894]	ATPase component	6.592	cell
hypothetical protein [*M. barkeri*]	ATPase component	100	cell
ABC transporter [*M. barkeri*]	ATPase component	specific	cell
hypothetical protein [*Microbacterium* sp. UCD-TDU]	ATPase component	5.473	cell
sugar ABC transporter ATP-binding protein [*Actinoplanes globisporus*]	ATPase component	specific	cell
iron ABC transporter ATP-binding protein [*Microbacterium* sp. UCD-TDU]	ATPase component	100	cell
ABC transporter ATP-binding protein [*Microbacterium* sp. UCD-TDU]	ATPase component	100	cell
branched-chain amino acid ABC transporter ATP-binding protein [*M. barkeri*]	ATPase component	3.332	cell
hypothetical protein [*M. barkeri*]	ATPase component	5.446	cell
hypothetical protein [*Actinopolymorpha alba*]	ATPase component	specific	cell
sugar ABC transporter ATP-binding protein [*M. barkeri*]	ATPase component	2.429	cell
hypothetical protein [*Microbacterium* sp. UCD-TDU]	ATPase component	100	cell
hypothetical protein [*Mycobacterium yongonense*]	ATPase component	2.266	cell
hypothetical protein [*Streptomyces* sp. AA0539]	ATPase component	specific	cell
iron-siderophore ABC transporter, substrate-binding protein [*Corynebacterium casei* UCMA 3821]	substrate-binding protein	100	extracellular
sugar ABC transporter substrate-binding protein [*Microbacterium* sp. UCD-TDU]	substrate-binding protein	3.66	extracellular
peptide ABC transporter substrate-binding protein [*Microbacterium* sp. UCD-TDU]	substrate-binding protein	specific	cell
ABC transporter substrate-binding protein [*M. barkeri*]	substrate-binding protein	11.788	extracellular
sugar ABC transporter substrate-binding protein [*Microbacterium laevaniformans*]	substrate-binding protein	100	extracellular
sugar ABC transporter substrate-binding protein [*M. barkeri*]	substrate-binding protein	specific	extracellular
ABC transporter permease [*Mycobacterium* sp. VKM Ac-1815D]	permease component	specific	cell
ABC transporter permease [*Microbacterium* sp. UCD-TDU]	permease component	specific	cell
ABC-type transporter, integral membrane subunit [*Isoptericola variabilis* 225]	permease component	specific	cell
ABC-type sugar transport systems, permease components [*M. testaceum* StLB037]	permease component	100	cell
binding-protein-dependent transport systems inner membrane component [*Beutenbergia cavernae* DSM 12333]	permease component	specific	cell
hypothetical protein [*Microbacterium* sp. 11MF]	permease component	100	cell
hypothetical protein [*Microbacterium* sp. UCD-TDU]	permease component	specific	cell
putative sugar ABC transporter permease protein [*Microlunatus phosphovorus* NM-1]	permease component	specific	cell
ABC transporter permease [*Microbacterium* sp. UCD-TDU]	permease component	specific	cell
thiamine ABC transporter ATP-binding protein [*Promicromonospora sukumoe*]	permease component	specific	cell
ABC transporter permease [*M. barkeri*]	permease component	specific	cell

DOI: 10.1021/acsomega.9b02313
ACS Omega 2019, 4, 19096−19105

Table 1. continued

protein name/Blast result	family	abundance ratio	identified location
hypothetical protein [*M. barkeri*]	permease component	2.077	cell
inner-membrane translocator [*Nocardioides* sp. CF8]	permease component	3.135	cell
ABC transporter permease [*Microbacterium* sp. UCD-TDU]	permease component	specific	cell

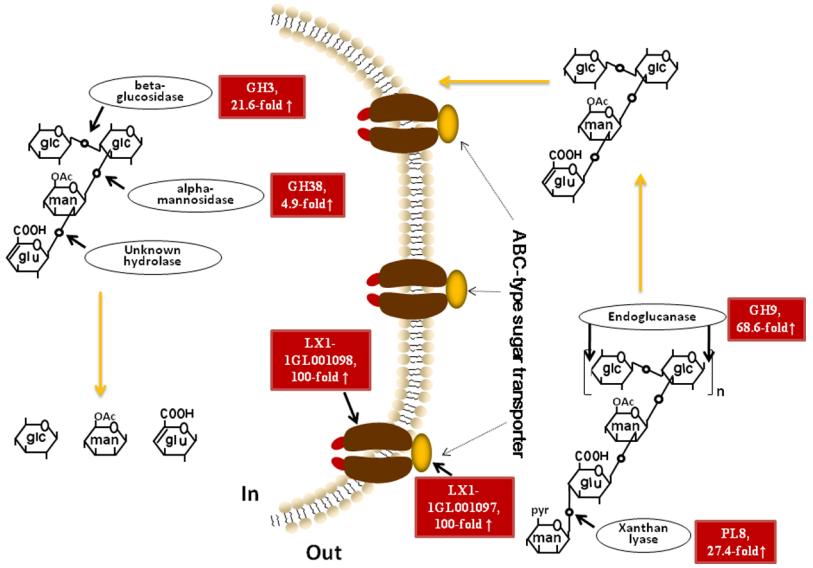

Figure 5. Schematic diagram showing a pathway for xanthan degradation and proteomic fold changes observed for all the catalytic enzymes and ABC-type sugar transporters.

depolymerization of xanthan in *Bacillus* sp. strain GL1 represented by Nankai et al.,[14] but the ABC-transporters participated in xanthan-degrading pathway were first detected. Moreover, these four CAZymes and an ABC-type sugar transport complex were not only identified by proteomic analysis but also confirmed as induced proteins when cultured in xanthan medium by quantitative results.

Quantitative Real-Time PCR and Enzyme Assay-Verified MS Analysis. To verify the MS screening results, we first measured the expression of 4 CAZymes (GH3, GH38, GH9, PL8) and 1 ABC transporter (LX1-1GL001097) in strain XT11 which was cultured in xanthan medium or glucose medium at the mRNA level using quantitative real-time PCR (qRT-PCR). As shown in Figure 6, the expression of GH3, GH38, GH9, PL8, and ABC was remarkably higher when cultured in xanthan medium than in glucose medium, which displayed the same tendency as indicated by the proteomic quantitative results (Supporting Information Table S5). As previously reported, MS analysis results were verified with quantitative real-time PCR.[32]

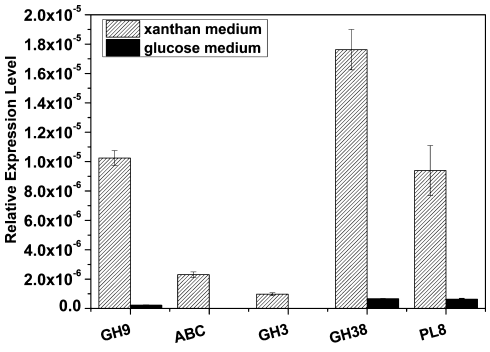

Figure 6. Bar graph showing the validation of proteomics screening results with qRT-PCR.

To further verify MS results, the functions of four CAZymes (GH3, GH38, GH9, and PL8) in the cluster were investigated. After heterologous expression and purification, the specific activity of GH3 toward pNPG, GH38 against pNP-α-D-man, GH9 and PL8 toward xanthan was 83.10 ± 2.23 U/g, 95.10 ± 11.06 U/g, 54.61 ± 6.12 U/g, 12.74 ± 0.13, respectively (Supporting Information Table S6, Figure S1), whereas when *Bacillus* sp. strain GL1 which is the first complete reported on xanthan degradation was cultured in xanthan medium, the activities of GH38, GH9, and PL8 were 0.060, 0.002, and 0.050 U/mL, respectively.[3,12,14] Therefore, compared with *Bacillus* sp. strain GL1, *Microbacterium* sp. XT11 showed greater xanthan-degrading ability. Meanwhile, the activities of four CAZymes in *Microbacterium* sp. XT11 cultured in xanthan medium and glucose medium were determined. When the strain XT11 was cultured in xanthan medium, the activities of GH3, GH38, GH9, and PL8 increased by 18.5-, 3.2-, 16.9-, and 2.5-folds (Figure 7), respectively, as compared with that in the glucose culture, indicating that all these four CAZymes in cluster were significantly induced by xanthan. All the results supported that these four CAZymes located in the same cluster should play a critical role the xanthan-degrading pathway in *Microbacterium* sp. XT11.

CONCLUSIONS

Using three different digestion strategies (trypsin, chymotrypsin, trypsin and chymotrypsin), 2746 and 2878 proteins were identified in proteomes of *Microbacterium* sp. XT11 in xanthan medium and glucose medium individually, which

DOI: 10.1021/acsomega.9b02313
ACS Omega 2019, 4, 19096−19105

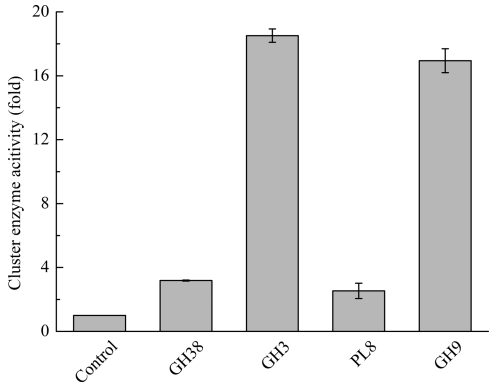

Figure 7. Bar graph showing the enzyme activity fold of 4 CAZymes (GH3, GH38, GH9, PL8) detected in xanthan medium. The enzyme activity of 4 CAZymes (GH3, GH38, GH9, PL8) detected in glucose medium was set as control to be 1.

represented 80.6 and 84.4% of total protein dataset expressed by the gene. Combining the up-regulated proteins quantified by the LFQ strategy and specifically expressed proteins in the xanthan medium, 430 proteins were considered as induced proteins related with xanthan biodegradation. Among these proteins, 19 proteins involved in CAZy and 38 proteins annotated with transporter activity were of potential significance in the degrading pathway of xanthan. Four CAZymes (GH3, GH38, GH9, and PL8) and one ABC transporter (LX1-1GL001097) were further verified with quantitative real-time PCR. Enzyme assay results of four CAZymes (GH3, GH38, GH9, and PL8) further supported the suggested xanthan-degrading pathway in *Microbacterium* sp. XT11. Finally, the knock-out of key enzymes or transporters will be carried out in our future work for in-depth investigation of the xanthan degrading pathway, and other identified induced proteins involved in CAZy or annotated with transporter activity were also needed for further investigation of their exact effect in the xanthan-degrading pathway.

MATERIAL AND METHODS

Chemicals and Materials. Trypsin and chymotrypsin were purchased from Sigma (USA). Chemical reagents of iodacetamine (IAA), 1, 4-dithiothreitol (DTT), trifluoroacetic acid (TFA), and formic acid (FA) were obtained from Sigma (USA). Water, acetonitrile, and methanol (optima-LC/MS grade) were obtained from Fisher Scientific (USA). Oasis HLB cartridges containing 10 mg of sorbent per cartridge with 30 μm of particle were purchased from Waters (USA). Steritop-GP filter units (0.22 μm) were obtained from Millipore (USA). The BCA protein quantitation kit was obtained from Beyotime Biotechnology (China). Other reagents used were all of analytical grade.

Microorganism and Culture Conditions. *Microbacterium* sp. XT11 was revived from cryo-preserved stocks stored at −80 °C and grew on Luria−Bertani (LB) agar plates. The single colony was inoculated into LB broth at 30 °C for 24 h. Then, the seed culture was transferred into xanthan medium and glucose medium, respectively. *Microbacterium* sp. XT11 was cultured in the xanthan medium at 30 °C as described elsewhere.[15] The xanthan medium consists of (per liter) 3 g of xanthan and 1 g of yeast extract in the mineral salt solution. The mineral salt solution contains (per liter) 250 mg of K_2HPO_4, 400 mg of NaCl, 125 mg of $MgSO_4{\cdot}7H_2O$, and 350 mg of KNO_3, and pH 7.0. 3 g glucose was used as the carbon source in place of xanthan in glucose medium.

Protein Extraction. Three batches of *Microbacterium* sp. XT11 were cultured for biological replicates. *Microbacterium* sp. XT11 started from the same frozen inoculum were cultured in the xanthan medium and glucose medium. Cultures for proteomic analysis were harvested at the middle of the exponential growth stage because xanthan solution was degraded obviously with significant decrease of viscosity in this period. The cell pellet was collected as cell fraction by centrifuging twice (5500*g*, 4 °C, 30 min). The supernatants were combined and filtered through a 0.22 μm membrane to obtain a cell-free fraction. Aliquots of 100 mL were processed using the trichloroacetic acid (TCA) method for proteomics analysis as follows. In brief, 100 mL of cell-free medium with 10 mL 100% (w/v) TCA added was vortexed for 15 s. After cooling in ice for at least 15 min, the mixture was centrifuged at 14 000*g* for 10 min at 4 °C and the supernatant was discarded. The pellet was washed twice with acetone and resuspended with buffer I (8 M urea + 50 mM Tris-HCl, pH 8.0). The protein concentration was determined by the BCA method and the resuspended sample was reserved at 80 °C for digestion.

For determining total protein production separately in the presence of xanthan or glucose, 50 mg (wet weight) of the cell pellet was washed thrice with PBS and resuspended in buffer II (8 M urea + 50 mM Tris-HCl + 0.1% Triton X-100, pH 8.0). Then, the cell pellet was disrupted by an ultrasonic cell discrupter (3 s with 3 s intervals for 180 times at 400 w). Finally, the supernatant was collected by centrifuging at 14 000*g* for 10 min at 4 °C and the concentration of proteins was determined by BCA assay.

Protein Digestion. Proteins (1 mg) in buffer I or buffer II was reduced with 10 mM DTT and alkylated with 20 mM IAA as previously reported.[33] Furthermore, the sample was diluted with 50 mM Tris-HCl and added with different enzymes (trypsin, chymotrypsin, or trypsin and chymotrypsin) with an enzyme to protein mass ratio of 1:50. After incubation at 37 °C overnight, the mixture was desalted by Oasis HLB cartridges and the eluate was lyophilized to dryness.

MS Analysis. After the lyophilized peptides were dissolved in 0.1% FA, the sample was loaded onto a reversed-phase μ-precolumn (C18PepMap100, 5 μm, 100 Å) and peptide separation was performed using a reversed-phase Acclaim PepMap RSLC analytical column (50 μm × 15 cm, 2 μm, 100 Å) by the Ultimate 3000 RSLCnano system (Dionex, USA) with a 200 nL/min flow rate. All the tests were performed in triplicate. The mobile phase was 0.1% FA/H_2O (A) and 80% ACN/0.1%FA/20% H_2O (B). For better separation, a gradient elution mode was used. The gradient set is as follows: 0 min, 4% B; 3 min, 10% B; 25 min, 35% B; 31 min, 55% B; 32 min, 95% B; 42 min, 95% B; 43 min, 4% B.

The resulting peptides were subjected to the nanoESI source followed by tandem mass spectrometry (MS/MS) in Q Exactive (Thermo Fisher Scientific, USA) coupled online to the UPLC. Intact peptides and ion fragments were detected in the Orbitrap at a resolution of 70 000 and 17 500 individually. Full-scan MS was acquired from m/z 350 to 1800. The MS/MS spectra were acquired in the data-dependent mode. The 15 most intense ions were selected for MS/MS with an automatic gain control target of 3×10^6. Normalized collision energy (27%) was used for the peptides selected for MS/MS. Ions (1

DOI: 10.1021/acsomega.9b02313
ACS Omega 2019, 4, 19096−19105

$\times 10^5$) were accumulated for generation of MS/MS spectra. Dynamic exclusion was set as 30.0 s. The electrospray voltage applied was 2.5 kV.

Data Analysis. The resulting MS/MS data were processed using Proteome Discoverer (version 2.2.0.388) with Sequent HT as the search engine. Tandem mass spectra were searched against DNA sequencing database of *Microbacterium* sp. XT11 (3409 sequences) concatenated with reverse decoy database. The false detection rate values for peptide identifications were controlled less than 1%. Trypsin (chymotrypsin, or trypsin and chymotrypsin) was specified as the cleavage enzyme allowing up to two missing cleavages. Mass error was set to 10 ppm for precursor ions and 0.02 Da for fragment ions. The minimum peptide length was set as 6 and maximum 144. Carbamidomethylation on Cys (+57.021 Da) was specified as static modification. Oxidation on Met (+15.995 Da) and acetylation on protein N-terminal (+42.011 Da) were set as dynamic modifications.

Total RNA Extraction and Real-Time PCR. RNA was extracted from strain XT11 cultured in xanthan medium or glucose medium using RNAiso Plus according to manufacturer's instruction (TaKaRa Bio, Japan). Totally 100 ng RNA was reverse-transcribed using the PrimeScript RT reagent Kit with gDNA Eraser (TaKaRaBio, Japan). The reverse transcription product was diluted to one-tenth and used as the template for quantitative real-time PCR (qRT-PCR) with TaKaRa PCR Thermal Cycler Dice Real Time System (TaKaRa Code. TP800). To normalize the cycle threshold values, the relative transcript level for 16S rDNA was determined. The condition used for qRT-PCR is as follows: 95 °C for 30 s, 35 cycles of 95 °C for 5 s, and 60 °C for 30 s. The primers used for qRT-PCR are listed in Table 2.

Table 2. List and Sequences of Primers Used for qRT-PCR Analysis

primer	sequence
qPCR-16S−F	5′-CCTGACTCTGGGATAAGCG-3′
qPCR-16S-R	5′-GAGCCATTACCTCACCAACAAG-3′
qPCR-glu-F	5′-GTACACCTGGGCGAATTG-3′
qPCR-glu-R	5′-TCTGGAAGAAGCGACCGAC-3′
qPCR-AB-F	5′-GAGATCACCACGAACAAC-3′
qPCR-AB-R	5′-TGAACGACGCCTTCCAGTC-3′
qPCR-Gco-F	5′-ACGCCTTGATCCCTACG-3′
qPCR-Gco-R	5′-ACATGAGCCCGACCTTCTC-3′
qPCR-man-F	5′-GTGGAGCCCGATACGAACATG-3′
qPCR-man-R	5′-TACCCGAAGGTGTCAGGGAG-3′
qPCR-xly-F	5′-TCAAGAGCAATGCCGACG-3′
qPCR-xly-R	5′-ATCTCATGGTGCCGAGGAC-3′

Heterologous Expression and Purification of Xanthan Degrading-Related Enzymes. Coding genes of GH3, GH38, GH9, and PL8 were amplified by PCR using the genomic DNA template extracted from *Microbacterium* sp. XT11 and ligated into the pET28a vector as described before.[17,30] The resulted recombinant plasmids were then transformed into electrocompetent *E. coli* BL21 (DE3) by electroporation. The recombinants were selected on LB plates containing 100 mg/L kanamycin. For induction, IPTG was added at a final concentration of 0.5 mM and the cells were further cultured at 16 °C for 12 h. Cells were disrupted by ultrasonic treatment. Following removal of cell debris by centrifugation, the supernatant was ready for subsequent purification. His-tagged GH3, GH38, GH9, and PL8 were respectively purified using a Ni-NTA purification system as described before.[34]

Enzyme Assay. For extracellular enzymes, the culture supernatant was used as crude enzyme solution. For intracellular enzymes, cells were harvested by centrifugation, and the cell pellet was suspended and sonicated using an ultrasonic processor (Branson Digital Sonifier; Branson, USA). Following removal of cell debris by centrifugation, the supernatant was ready for subsequent enzyme assay. For heterologously expressed enzymes, purified proteins were assayed.

The specific activity of the endoglucanase was determined by incubating 5 g/L xanthan with crude enzyme solution in 10 mM NaH_2PO_4−Na_2HPO_4 buffer (pH 7.5). The reaction was conducted at 40 °C for 20 min and then terminated by boiling the mixture for 5 min. The liberation of reducing end sugars was assayed by the 2, 2′-bicinchoninate method. One unit of enzyme activity was defined as the amount of enzyme that produced 1 μmol reducing end sugar per min.

The activity of xanthan lyase was assayed in the reaction mixture containing 0.5 g/L xanthan in 100 mM potassium phosphate buffer (pH 6.0) and appropriately diluted crude enzyme solution. After incubation at 40 °C for 10 min, the increase in the absorbance at 235 nm was determined. One unit of xanthan lyase activity was defined as the amount of enzyme that produced an increase of 1.0 in the absorbance at 235 nm per min under the above condition.

To measure the activity of beta-glucosidase toward *p*-nitrophenyl β-D-glucopyranoside (pNPG), the reaction mixture containing 2.5 mM pNPG and appropriately diluted crude enzyme in 50 mM sodium phosphate buffer (pH 7.0) were incubated for 10 min at 40 °C and stopped by the addition of 0.5 mL of 1 M Na_2CO_3. The absorbance of the mixture was measured at 405 nm. One unit of enzyme activity was defined as the amount to liberate 1 μM of *p*-nitrophenol (pNP) per min under the assay conditions.

The activity of alpha-mannosidase toward *p*-nitrophenyl a-D-mannopyranoside (pNP-α-D-man) was measured by incubating 0.4 mM pNP-α-D-man and appropriately diluted crude enzyme in 50 mM sodium phosphate buffer (pH 7.0). The reaction was carried out at 40 °C for 10 min and then terminated by adding 0.4 mL of 0.25 M Na_2CO_3. The absorbance at 405 nm was determined. One unit of enzyme activity was defined as the amount to liberate 1 μM of *p*-nitrophenol (pNP) per min under the assay conditions.

All the assays were conducted in triplicate, and the mean values were presented.

■ ASSOCIATED CONTENT

Supporting Information

The Supporting Information is available free of charge on the ACS Publications website at DOI: 10.1021/acsomega.9b02313.

SDS-PAGE analysis of purified enzymes; enzyme activities in the supernatant and cell extract of different *Microbacterium* sp. XT11 cultures; relative transcriptional levels of xanthan degradation-related proteins in *Microbacterium* sp. XT11 cultured in different media (PDF)

The detailed information of 229 proteins which were specifically expressed in the identified 2746 proteins of proteome I. The detailed information of 361 proteins

DOI: 10.1021/acsomega.9b02313
ACS Omega 2019, 4, 19096−19105

which were specifically expressed in the identified 2878 proteins of proteome II. The detailed information of 179 higher expression cell proteins which showed a twofold change in abundance compared to the control. The detailed information of 36 higher expression extracellular proteins which showed a twofold change in abundance compared to the control (XLSX)

AUTHOR INFORMATION

Corresponding Authors

*E-mail: yangfan@dlpu.edu.cn (F.Y.).
*E-mail: xianzhen@mail.com (X.L.).

ORCID

Xianzhen Li: 0000-0003-0191-9484

Author Contributions

†H.L. and X.W. have contributed equally to this work.

Notes

The authors declare no competing financial interest.

ACKNOWLEDGMENTS

Z.S. and F.Y. received funding from Natural Sciences Foundation of China (31601458, 31671796). Z.S. received funding from Doctoral Start-up Foundation of Liaoning Province (201601272). F.Y. received funding from Liaoning BaiQianWan Talents Program. Z.S. received funding from High Level Talent Innovation and Entrepreneurship Program Supported by Dalian (2017RQ054).

REFERENCES

(1) García-Ochoa, F.; Santos, V. E.; Casas, J. A.; Gómez, E. Xanthan gum: production, recovery, and properties. *Biotechnol. Adv.* **2000**, *18*, 549−579.

(2) Jansson, P.-e.; Kenne, L.; Lindberg, B. Structure of the extracellular polysaccharide from Xanthomonas campestris. *Carbohydr. Res.* **1975**, *45*, 275−282.

(3) Nankai, H.; Hashimoto, W.; Murata, K. Molecular identification of family 38 -mannosidase of Bacillus sp. strain GL1, responsible for complete depolymerization of xanthan. *Appl. Environ. Microbiol.* **2002**, *68*, 2731−2736.

(4) Savvides, A. L.; Katsifas, E. A.; Hatzinikolaou, D. G.; Karagouni, A. D. Xanthan production by Xanthomonas campestris using whey permeate medium. *World J. Microbiol. Biotechnol.* **2012**, *28*, 2759−2764.

(5) Xu, L.; Xu, G.; Liu, T.; Chen, Y.; Gong, H. The comparison of rheological properties of aqueous welan gum and xanthan gum solutions. *Carbohydr. Polym.* **2013**, *92*, 516−522.

(6) Khalil, M.; Mohamed Jan, B. Herschel-Bulkley rheological parameters of a novel environmentally friendly lightweight biopolymer drilling fluid fromxanthan gumand starch. *J. Appl. Polym. Sci.* **2012**, *124*, 595−606.

(7) Daniels, M. J.; Collinge, D. B.; Dow, J. M.; Osbourn, A. E.; Roberts, I. N. Molecular biology of the interaction of Xanthomonas campestris with plants. *Plant Physiol. Biochem.* **1987**, *25*, 353−359.

(8) Liu, H.; Huang, C.; Dong, W.; Du, Y.; Bai, X.; Li, X. Biodegradation of xanthan by newly isolated Cellulomonas, sp. LX, releasing elicitor-active xantho-oligosaccharides-induced phytoalexin synthesis in soybean cotyledons. *Process Biochem.* **2005**, *40*, 3701−3706.

(9) Levy, S.; Schuyler, S. C.; Maglothin, R. K.; Staehelin, L. A. Dynamic simulations of the molecular conformations of wild type and mutant xanthan polymers suggest that conformational differences may contribute to observed differences in viscosity. *Biopolymers* **1996**, *38*, 251−272.

(10) Cadmus, M. C.; Jackson, L. K.; Burton, K. A.; Plattner, R. D.; Slodki, M. E. Biodegradation of xanthan gum by *Bacillus* sp. *Appl. Environ. Microbiol.* **1982**, *44*, 5−11.

(11) Ruijssenaars, H. J.; De Bont, J. A. M.; Hartmans, S. A. Pyruvated Mannose-Specific Xanthan Lyase Involved in Xanthan Degradation by Paenibacillus alginolyticus XL-1. *Appl. Environ. Microbiol.* **1999**, *65*, 2446−2452.

(12) Hashimoto, W.; Miki, H.; Tsuchiya, N.; Naikai, H.; Murata, K. Xanthan lyase of Bacillus sp. strain GL1 liberates pyruvylated mannose from xanthan side chains. *Appl. Environ. Microbiol.* **1998**, *64*, 3765−3768.

(13) Moroz, O. V.; Jensen, P. F.; McDonald, S. P.; Wilson, K. S.; McGregor, N.; Blagova, E.; Comamala, G.; Segura, D. R.; Anderson, L.; Vasu, S. M.; Rao, V. P.; Giger, L.; Sørensen, T. H.; Monrad, R. N.; Svendsen, A.; Nielsen, J. E.; Henrissat, B.; Davies, G. J.; Brumer, H.; Rand, K. D.; Wilson, K. S. Structural Dynamics and Catalytic Properties of a Multimodular Xanthanase. *ACS Catal.* **2018**, *8*, 6021−6034.

(14) Nankai, H.; Hashimoto, W.; Miki, H.; Kawai, S.; Murata, K. Microbial System for Polysaccharide Depolymerization: Enzymatic Route for Xanthan Depolymerization by Bacillus sp. Strain GL1. *Appl. Environ. Microbiol.* **1999**, *65*, 2520−2526.

(15) Qian, F.; An, L.; Wang, M.; Li, C.; Li, X. Isolation and characterization of a xanthan-degrading Microbacterium sp. strain XT11 from garden soil. *J. Appl. Microbiol.* **2007**, *102*, 1362−1371.

(16) Li, B.; Guo, J.; Chen, W.; Chen, X.; Chen, L.; Liu, Z.; Li, X. Endoxanthanase, a novel -d-Glucanase hydrolyzing backbone linkage of intact xanthan from newly isolated Microbacterium sp. XT11. *Appl. Biochem. Biotechnol.* **2009**, *159*, 24−32.

(17) Yang, F.; Yang, L.; Guo, X.; Wang, X.; Li, L.; Liu, Z.; Wang, W.; Li, X. Production and Purification of a Novel Xanthan Lyase from a Xanthan-Degrading Microbacterium sp. Strain XT11. *Sci. World J.* **2014**, *2014*, 368−434.

(18) Yang, F.; Li, L.; Si, Y.; Yang, M.; Guo, X.; Hou, Y.; Chen, X.; Li, X. Complete genome sequence of a xanthan-degrading Microbacterium sp. strain XT11 with the potential for xantho-oligosaccharides production. *J. Biotechnol.* **2016**, *222*, 19−20.

(19) Fry, S. C.; Aldington, S.; Hetherington, P. R.; Aitken, J. Oligosaccharides as signals and substrateds in the plant wall. *Plant Physiol.* **1993**, *103*, 1−5.

(20) Gstaiger, M.; Aebersold, R. Applying mass spectrometry-based proteomics to genetics, genomics and network biology. *Nat. Rev. Genet.* **2009**, *10*, 617−627.

(21) Han, X.; Aslanian, A.; Yates, J. R. Mass spectrometry for proteomics. *Curr. Opin. Chem. Biol.* **2008**, *12*, 483−490.

(22) Smith, J. C.; Figeys, D. Proteomics technology in systems biology. *Mol. Biosyst.* **2006**, *2*, 364−370.

(23) Steen, H.; Mann, M. The ABC's (and XYZ's) of peptide sequencing. *Nat. Rev. Mol. Cell Biol.* **2004**, *5*, 699−711.

(24) Biringer, R. G.; Amato, H.; Harrington, M. G.; Fonteh, A. N.; Riggins, J. N.; Hühmer, A. F. R. Enhanced sequence coverage of proteins in human cerebrospinal fluid using multiple enzymatic digestion and linear ion trap LC-MS/MS. *Briefings Funct. Genomics Proteomics* **2006**, *5*, 144−153.

(25) Swaney, D. L.; Wenger, C. D.; Coon, J. J. Value of Using Multiple Proteases for Large-Scale Mass Spectrometry-Based Proteomics. *J. Proteome Res.* **2010**, *9*, 1323−1329.

(26) Petersen, T. N.; Brunak, S.; von Heijne, G.; Nielsen, H. SignalP 4.0: discriminating signal peptides from transmembrane regions. *Nat. Methods* **2011**, *8*, 785−786.

(27) Cox, J.; Hein, M. Y.; Luber, C. A.; Paron, I.; Nagaraj, N.; Mann, M. Accurate proteome-wide label-free quantification by delayed normalization and maximal peptide ratio extraction, termed MaxLFQ. *Mol. Cell. Proteomics* **2014**, *13*, 2513−2526.

(28) Ye, J.; Fang, L.; Zheng, H.; Zhang, Y.; Chen, J.; Zhang, Z.; Wang, J.; Li, S.; Li, R.; Bolund, L.; Wang, J. WEGO: a web tool for plotting GO annotations. *Nucleic Acids Res.* **2006**, *34*, W293−W297.

(29) Altschul, S. F.; Gish, W.; Miller, W.; Myers, E. W.; Lipman, D. J. Basic local alignment search tool. *J. Mol. Biol.* **1990**, *215*, 403−410.

DOI: 10.1021/acsomega.9b02313
ACS Omega 2019, 4, 19096−19105

(30) Yang, F.; Li, H.; Sun, J.; Guo, X.; Zhang, X.; Tao, M.; Chen, X.; Li, X. Novel Endotype Xanthanase from Xanthan-Degrading Microbacterium sp. Strain XT11. *Appl. Environ. Microbiol.* **2018**, *85*, e01800−01818.
(31) Eitinger, T.; Rodionov, D. A.; Grote, M.; Schneider, E. Canonical and ECF-type ATP-binding cassette importers in prokaryotes: diversity in modular organization and cellular functions. *FEMS Microbiol. Rev.* **2011**, *35*, 3−67.
(32) Sun, Z.; Dong, J.; Zhang, S.; Hu, Z.; Cheng, K.; Li, K.; Xu, B.; Ye, M.; Nie, Y.; Fan, D.; Zou, H. Identification of Chemoresistance-Related Cell-Surface Glycoproteins in Leukemia Cells and Functional Validation of Candidate Glycoproteins. *J. Proteome Res.* **2014**, *13*, 1593−1601.
(33) Wang, F.; Dong, J.; Jiang, X.; Ye, M.; Zou, H. Capillary trap column with strong cation-exchange monolith for automated shotgun proteome analysis. *Anal. Chem.* **2007**, *79*, 6599−6606.
(34) Crowe, J.; Döbeli, H.; Gentz, R.; Hochuli, E.; Stüber, D.; Henco, K. 6xHis-Ni-NTA chromatography as a superior technique in recombinant protein expression/purification. *Methods Mol. Biol.* **1994**, *31*, 371−387.

DOI: 10.1021/acsomega.9b02313
ACS Omega 2019, 4, 19096−19105